Semiempirical amplitude analysis of $\gamma + p \to \pi^0 + p$ from incomplete data at high energies

M. Svec
Physics Department, McGill University, Montreal, P.Q., Canada
(Received 16 May 1979)

Fixed-t dispersion relations together with an effective Regge-pole parametrization of exchange amplitudes are used to transform the incomplete high-energy data into information about amplitudes. Clear trends in the t structure and energy dependence emerge in the two obtained solutions corresponding to a discrete ambiguity. The sensitivity of the solutions on polarization and low-energy inputs is investigated in great detail with important conclusions about the t structure of amplitudes. In solution I, $\mathrm{Im}H_n$ is peripheral but $\mathrm{Im}H_0$ is sensitive to polarization input for $-t \lesssim 0.3$ GeV^2. The single-flip amplitude cannot be described as a simple Regge pole in contrast to πN charge exchange. In solution II, only $\mathrm{Im}H_1$ is peripheral and the structures of $\mathrm{Im}H_0$ and $\mathrm{Im}H_2$ are approximately reversed. Solution II is tentatively rejected. It is also found that the t structure of amplitudes and their energy dependence are only weakly related. Our solutions are compared with results obtained by other authors and we comment also on the observed absorption effects.

I. INTRODUCTION

In recent years much of the interest in two-body hadronic reactions has focused on obtaining information about the t structure and energy dependence of exchange amplitudes directly from available data. The photoproduction of the π^0 meson on nucleon provides an opportunity to examine exchange amplitudes which do not participate in the simpler pseudoscalar-nucleon reactions. This reaction can be described in terms of four complex s-channel helicity amplitudes (SHA's) $H_n(s,t)$, $n=0,\ 1,\ 1',\ 2$ so that different helicity configurations are also involved. The SHA's receive contributions from natural and unnatural exchanges: In addition to ω and ρ exchanges, the contribution from B exchange is also important. The experimental effective trajectory is rather small and deviates significantly from linear α_ρ and α_ω trajectories, a feature which adds to the interest in this reaction.

Direct amplitude analysis of π^0 photoproduction requires a complete set of data which consists of seven independent observables. Their best choice has been discussed in the literature.[1-4] Additional two double-polarization measurements are needed to remove discrete ambiguities.[4] So far only the differential cross section $d\sigma/dt$ (Refs. 5–7), polarized-photon asymmetry A (Ref. 6), polarized-target asymmetry T (Refs. 8 and 9), and recoil-nucleon polarization P (Ref. 10) have been measured at high energies. A proposal has been made to measure double-polarization parameters.[11]

In the absence of a complete set of data, fixed-t dispersion relations (FTDR's) were used by various authors[12-15] to obtain pion photoproduction amplitudes from the incomplete data. In addition to information about the low-energy amplitudes, a parametrization of the imaginary parts of amplitudes at high energies is required. The least model-dependent analysis is that of Argyres *et al.*[13] and their work provided the first amplitude analysis of $\gamma p \to \pi^0 p$. Their method reduces the number of required polarization experiments by half. FTDR's were used also for amplitude analyses of πN charge-exchange (CEX), KN charge-exchange (CEX), and hypercharge-exchange reactions. These efforts were reviewed in detail by Contogouris.[16] Most recently FTDR's were used in an amplitude analysis of $\pi^- p \to \eta n$.[17]

In this paper we expand on our previous work[13] and present a new amplitude analysis of π^0 photoproduction. The analysis is based on FTDR's and on effective Regee-pole parametrization of imaginary parts of exchange amplitudes. The high-energy data known over a range of energies are transformed, t by t, into information about the effective Regge residue and effective Regge trajectory for each exchange amplitude. The SHA's are then simply reconstructed. This semiempirical approach to construction of amplitudes from incomplete data allows us to examine both the t structure and s dependence of individual amplitudes if sufficient high-energy information is available. We address ourselves also to the study of certain ambiguities in the solutions, their sensitivity to input data, and stability of their structure. A similar analysis of πN CEX up to 200 GeV has been published.[18]

The paper is organized as follows. In Sec. II we present the basic formalism and discuss the method for construction of amplitudes. The input data are reviewed in Sec. III. In Sec. IV we concentrate on unnatural amplitudes and motivate simplifications in their treatment. Analysis with one linear effective trajectory is presented in Sec. V and its deficiency in the energy dependence

is discussed. In Sec. VI we present amplitudes obtained in the analysis with independent effective trajectories. Throughout this work two different low-energy partial-wave analyses and three different polarization inputs were used in order to determine sensitivity of the solutions for amplitudes on this input. Uniqueness of the final solution is also examined. Predictions for single- and double-polarization parameters are given in Sec. VII. In Sec. VIII we comment further on some features of the obtained amplitudes, compare them with results of other authors, and comment on the absorption effects in π^0 photoproduction. Our results are summarized in Sec. IX.

II. PRESENTATION OF THE METHOD

A. Kinematics and FTDR's

The measured observables $d\sigma/dt$, A, T, P can be expressed in terms of the four SHA's as follows:

$$\frac{d\sigma}{dt} = |H_0|^2 + |H_1|^2 + |H_1'|^2 + |H_2|^2, \tag{1a}$$

$$A\frac{d\sigma}{dt} = 2\,\mathrm{Re}(H_1'H_1^* - H_0H_2^*), \tag{1b}$$

$$T\frac{d\sigma}{dt} = 2\,\mathrm{Im}(H_1'H_0^* - H_1H_2^*), \tag{1c}$$

$$P\frac{d\sigma}{dt} = 2\,\mathrm{Im}(H_1H_0^* - H_1'H_2^*). \tag{1d}$$

Here H_0 is nonflip, H_1, H_1' single-flip, and H_2 double-flip amplitudes.

It is now useful to introduce the following combinations of SHA:

$$H_1 = N_1 + U_1, \quad H_1' = N_1 - U_1, \tag{2a}$$

$$H_0 = N_0 + U_0, \quad H_2 = -N_0 + U_0. \tag{2b}$$

These new amplitudes conserve naturality at high energies (to the leading order in s[19]), where the amplitudes N_n and U_n, $n=0,1$ are natural and unnatural amplitudes, respectively. The observables (1) can be expressed in terms of these amplitudes but it is more helpful to introduce new combinations of observables

$$\sigma_N = \tfrac{1}{2}(1+A)\frac{d\sigma}{dt}, \quad \sigma_U = \tfrac{1}{2}(1-A)\frac{d\sigma}{dt}, \tag{3a}$$

$$P_N = \tfrac{1}{2}(P+T)\frac{d\sigma}{dt}, \quad P_U = \tfrac{1}{2}(P-T)\frac{d\sigma}{dt}. \tag{3b}$$

Then

$$\sigma_N = 2(|N_0|^2 + |N_1|^2), \tag{4a}$$

$$P_N = -4\,\mathrm{Im}(N_0N_1^*), \tag{4b}$$

$$\sigma_U = 2(|U_0|^2 + |U_1|^2), \tag{5a}$$

$$P_U = -4\,\mathrm{Im}(U_0U_1^*). \tag{5b}$$

The observables (1) now separate into two independent sets of equations for a separate determination of natural and unnatural amplitudes. We note that Eqs. (4) and (5) are analogous to those for πN CEX amplitudes.

Although our purpose is to study the SHA's $H_n(\nu, t)$, $n=0, 1, 1', 2,$ the definite-naturality amplitudes (DNA's) N_n and U_n, $n=0,1$ serve as a useful intermediate step. However, any unresolved ambiguity in the solution of any one of these sets of equations will generate also an ambiguity in the solutions for the SHA's H_n.

For large energies the DNA's can be simply expressed in terms of the Chew-Goldberger-Low-Nambu (CGLN) invariant amplitudes A_i $i=1,2,3,4$ (Ref. 20):

$$N_0 = 2kA_1, \quad N_1 = -k\sqrt{-t}A_4, \tag{6}$$

$$U_0 = 2k(A_1 + tA_2), \quad U_1 = -k\sqrt{-t}A_3, \tag{7}$$

where $k = 1/4\sqrt{2}\pi$. For $\gamma p \to \pi^0 p$ the amplitudes A_i are expressed in terms of the CGLN isospin combination[20]

$$A_i = A_i^{(+)} + A_i^{(0)}, \quad i=1,\ldots,4. \tag{8}$$

For $i=1$, 2, and 4 the amplitudes $A_i^{(+)}$ and $A_i^{(0)}$ are crossing even while $A_3^{(+)}$ and $A_3^{(0)}$ are crossing odd. The dispersion relations for $A_i^{(+)} + A_i^{(0)}$ therefore imply similar FTDR's for amplitudes N_n and U_n, $n=0,1$, which are valid at high energies ($k_{\mathrm{lab}} \gtrsim 3$ GeV) where the approximation of exact DNA's in terms of expressions (6) and (7) is good.

The natural amplitudes N_n, $n=0,1$ then satisfy FTDR's

$$\mathrm{Re}N_n(\nu,t) = r_n^{(N)}\frac{2\nu_B}{\nu_B^2 - \nu^2} + \frac{2}{\pi}\mathrm{P}\int_{\nu_0}^{+\infty} d\nu' \frac{\nu'\,\mathrm{Im}N_n(\nu',t)}{\nu'^2 - \nu^2}. \tag{9}$$

The crossing-even amplitude $U_0(\nu, t)$ satisfies a FTDR similar to Eq. (9). The FTDR for the crossing-odd amplitude $U_1(\nu, t)$ reads

$$\mathrm{Re}U_1(\nu,t) = r_1^{(U)}\frac{2\nu}{\nu_B^2 - \nu^2} + \frac{2\nu}{\pi}\mathrm{P}\int_{\nu_0}^{+\infty} d\nu' \frac{\mathrm{Im}U_1(\nu',t)}{\nu'^2 - \nu^2}. \tag{10}$$

Here

$$\nu_B = (t-\mu^2)/4M, \quad \nu_0 = \mu + (t+\mu^2)/4M,$$

and $\nu = (s-u)/4\mathrm{M}$, M = mass of nucleon. The pole residues $r_n^{(N)}$ and $r_n^{(U)}$ are easily determined in terms of the residues of A_i.[20,21]

B. Effective Regge-poles analysis

We consider first the natural amplitudes. The

dispersion integrals are split into a low-energy part $\nu_0 < \nu' < N$, and a high-energy part $\nu' > N$. The cutoff energy N is determined by the partial-wave analysis used to evaluate the low-energy part of FTDR. For $\nu > N$ we assume

$$\mathrm{Im}N_n(\nu, t) = \beta_n(t)\nu^{\alpha_n(t)-1}, \quad n = 0, 1. \tag{11}$$

Using the well-known Hilbert transform, we obtain for the real parts[13]

$$\mathrm{Re}N_n(\nu, t) = \tan\left(\frac{\pi}{2}\alpha_n\right)\mathrm{Im}N_n(\nu, t) + \gamma_n^{(N)}\frac{2\nu_B}{\nu_B^2 - \nu^2} + \frac{2}{\pi}\int_{\nu_0}^{N} d\nu' \frac{\nu'[\mathrm{Im}N_n(\nu', t) - \beta_n(t)\nu'^{\alpha_n - 1}}{\nu^2 - \nu'^2}. \tag{12}$$

Expanding in powers of $1/\nu^2$ and retaining only the first terms we get for $\nu > N' > N$ ($N' \gtrsim 3$ GeV)

$$\mathrm{Re}N_n(\nu, t) = \rho_n(\nu, t)\,\mathrm{Im}N_n(\nu, t) + \frac{1}{\nu^2}Q_n^{(N)}(t), \tag{13}$$

where

$$\rho_n(\nu, t) = \tan\left(\frac{\pi}{2}\alpha_n\right) + \frac{2}{\pi}\frac{1}{1+\alpha_n}\left(\frac{N}{\nu}\right)^{1+\alpha_n} \tag{14}$$

and

$$Q_n^{(N)}(t) = -2\gamma_n^{(N)}\nu_B - \frac{2}{\pi}\int_{\nu_0}^{N} d\nu'\,\nu'\,\mathrm{Im}N_n(\nu', t). \tag{15}$$

Substituting Eqs. (11) and (13) into Eq. (4b) we obtain a relation

$$\mathrm{Im}N_0(\nu, t) = \frac{Q_0^{(N)}(t)\,\mathrm{Im}N_1(\nu, t) - \frac{1}{4}\nu^2 P_N(\nu, t)}{(\rho_1 - \rho_0)\nu^2\,\mathrm{Im}N_1(\nu, t) + Q_1^{(N)}(t)}, \tag{16}$$

which is used to transform Eq. (4a) into a fourth-order algebraic equation for $\mathrm{Im}N_1$ (or β_1). With the experimental data for $d\sigma/dt$, A, P, T known at 4 GeV, the equation for $\mathrm{Im}N_1$ (β_1) can be solved at each value of t but an assumption about α_0 and α_1 must be made and reasonable criteria for selection of a physical solution must be specified.

In our approach we search, t by t, for values of α_0 and α_1 which produce a solution for N_0 and N_1 with the following properties: (i) $\mathrm{Im}N_1(\nu, t)$ has qualitative features of $\mathrm{Im}N_1$ at the cutoff energy N (continuity in energy). (ii) The solution fits the available data on σ_N at higher energies. (iii) Taken together with the solution for unnatural amplitudes, the resulting predictions for $d\sigma/dt$ and A at higher energies are within experimental errors. (iv) The amplitudes vary smoothly as functions of t.

For the unnatural amplitudes U_n we also assume

$$\mathrm{Im}U_n(\nu, t) = \bar{\beta}_n(t)\nu^{\bar{\alpha}_n(t)-1}, \quad n = 0, 1, \tag{17}$$

for $\nu > N$. Expressions corresponding to Eqs. (12)–(16) can now be written and one can consider determination of $\mathrm{Im}U_n$ from σ_U and P_U in a manner similar to determination of the natural amplitudes. We discuss the unnatural amplitudes in more detail in Sec. IV after we review the input information in Sec. III. In particular we motivate a simplification of the present analysis, namely assumptions that $U_1(\nu, t) = 0$ for $k_{1\,\mathrm{ab}} \gtrsim 4$ GeV and $\bar{\alpha}_0 = \alpha_0$.

In Eqs. (11) and (17) we have implicitly assumed that

$$\alpha_n^{(+)} = \alpha_n^{(0)} \text{ and } \bar{\alpha}_n^{(+)} = \bar{\alpha}_n^{(0)}, \quad n = 0, 1, \tag{18}$$

i.e., weak $\omega - \rho$ and A_1-B exchange degeneracy in $\gamma p \to \pi^0 p$. We are forced into this approximation since there are no data on P and T polarizations in the $\gamma n \to \pi^0 n$ reaction at high energies. The isotopic separation of the exchange amplitudes in π^0 photoproduction is thus not yet possible.

III. EVALUATION OF THE INPUT DATA

The first multipole analyses of $\gamma p \to \pi^0 p$ extending into the third resonance region[22-24] have been followed recently by four analyses[25-29] each using a different approach in their attempts to improve the previous results and also explore the fourth resonance region.

The analyses of Moorhouse *et al.* (MOR)[25] and

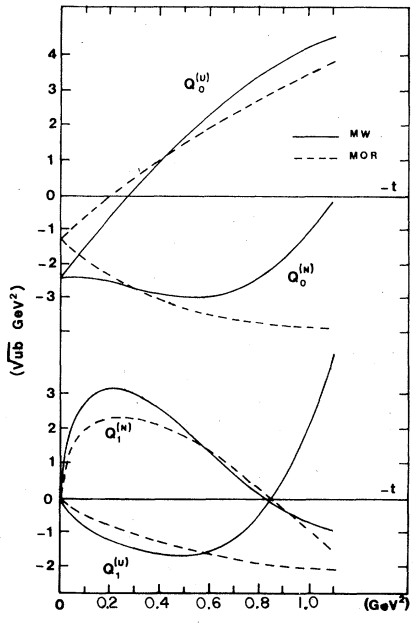

FIG. 1. The low-energy contributions $Q_n^{(N)}$ and $Q_n^{(U)}$, $n = 0, 1$. Full lines—analysis of Metcalf and Walker (Ref. 28); dashed lines—analysis of Moorhouse, Oberlack, and Rosenfeld (Ref. 25).

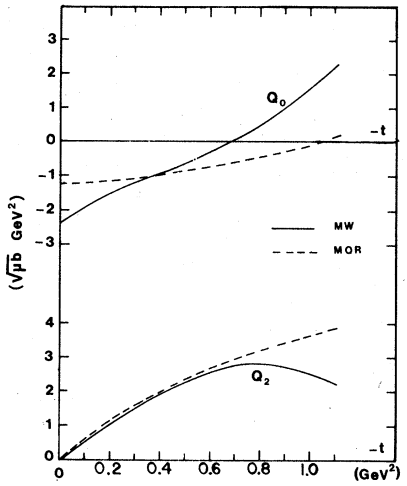

FIG. 2. The low-energy contributions Q_0 and Q_2. The notation as in Fig. 1.

its extension by Knies *et al.* (KMO),[26] Devenish *et al.* (DLR),[27] and Crawford[29] all use FTDR's but differ in their treatment of the high-energy part of dispersion integrals and also in their parametrization of the low-energy imaginary parts of the amplitudes. In contrast, Metcalf and Walker (MW)[28] do not use FTDR's. The analysis of MOR extends to k_{1ab} $=1.2$ GeV; the other analyses extend to $k_{1ab}=1.7$ GeV. All analyses agree quite well for the first- and second-resonance-region γN couplings, except for the neutral $P11(1434)$. The situation in the third and fourth resonance region is, however,

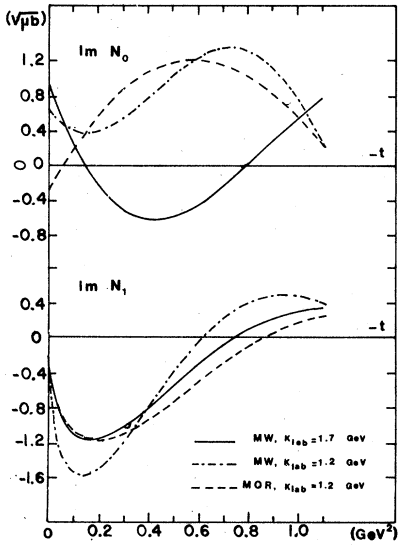

FIG. 3. The behavior of $\mathrm{Im}N_0$ and $\mathrm{Im}N_1$ at the cut-off energies. Solid and dash-dotted lines—analysis of Metcalf and Walker (Ref. 28) at k_{1ab}=1.7 and 1.2 GeV, respectively. Dashed lines— analysis of Moorhouse, Oberlack, and Rosenfeld (Ref. 25) at $k_{1ab}=1.2$ GeV.

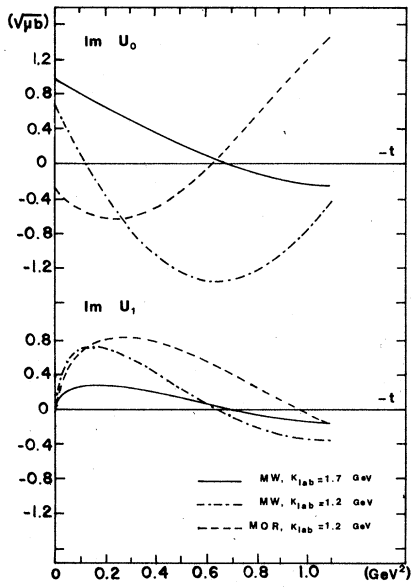

FIG. 4. The behavior of $\mathrm{Im}U_0$ and $\mathrm{Im}U_1$ at the cutoff energies. Notation as in Fig. 3.

still very uncertain.[30] The quality of the fit to their respective data sets is best for the MW solution and worst for the DLR solution. This is to be expected since MW have the least and DLR the most constrained background amplitudes.

In our analysis we worked with the low-energy parts of FTDR's calculated on the basis of the Metcalf and Walker analysis[28] and the Moorhouse, Oberlack, and Rosenfeld analysis.[25] The two corresponding sets will be referred to as Q(MW)

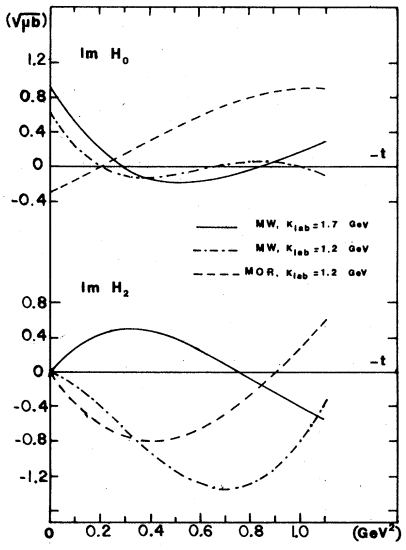

FIG. 5. The behavior of $\mathrm{Im}H_0$ and $\mathrm{Im}H_2$ at the cutoff energies. Notation as in Fig. 3.

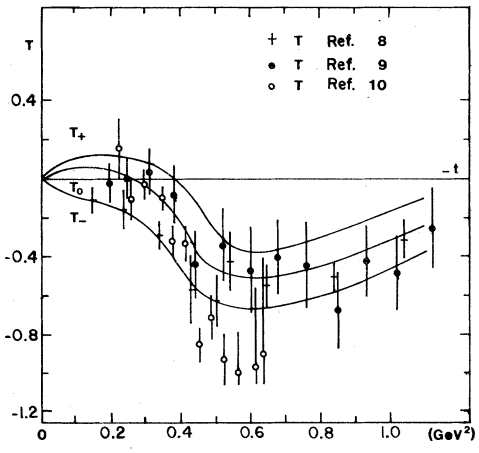

FIG. 6. The data on polarized-target asymmetry T and recoil polarization P. The curves T_+, T_0, and T_- are the three inputs used in this analysis.

and Q(MOR). They are shown in Fig. 1 for the natural and unnatural amplitudes N_n and U_n, $n=0, 1$, and in Fig. 2 for the SHA's H_0 and H_2. We notice that the largest differences occur in $Q_0^{(N)}$, Q_0, and $Q_1^{(U)}$.

In Figs. 3–5 we compare $\mathrm{Im}N_n$, $\mathrm{Im}U_n$, $n=0, 1$ and $\mathrm{Im}H_n$, $n=0, 2$ of the two analyses at $k_{1\mathrm{ab}}=1.2$ GeV and present also MW results at $k_{1\mathrm{ab}}=1.7$ GeV. We notice that $\mathrm{Im}H_0$ of the two analyses have opposite signs for $-t \lesssim 0.6$ GeV^2 but the positions of their first zero are close and consistent with a "J_0" t structure. Also, $\mathrm{Im}H_2$ at 1.7 GeV has an opposite sign relative to $\mathrm{Im}H_2$ at 1.2 GeV of both analysis. Results for $\mathrm{Im}N_0$ and $\mathrm{Im}U_0$ show similar sign differences between the two analyses. Because of the large uncertainties in the behavior of these amplitudes at cutoff energies, we will base the selection of solutions in our analysis only on the behavior of $\mathrm{Im}N_1$.

The high-energy input data necessary to carry out our analysis—$d\sigma/dt$, A, T, P— were measured at 4 GeV. For $d\sigma/dt$ we took the most recent DESY data[7] and for A the SLAC results.[6] In Fig. 6 we show the data for polarized-target symmetry T (Refs. 8 and 9) at 4 GeV and the results for recoil-nucleon polarization P between 3 and 7 GeV.[10] In view of the large errors we used in the actual analysis three polarization inputs T_+, T_0, T_- as represented in Fig. 6. We also fitted the SLAC data on $d\sigma/dt$ at 6, 9, 12, and 15 GeV and A at 6 and 10 GeV.[6]

IV. THE UNNATURAL AMPLITUDES

The Eqs. (5) for the unnatural amplitudes can be greatly simplified. The well-known expressions of the invariant amplitudes A_i in terms of the parity-conserving t-channel helicity amplitudes[31] show that A_3, i.e., U_1, is dominated by t-channel exchanges with exotic quantum numbers $P(-)^J = C(-)^J = -1$ (P = parity, J = spin, C = charge-conjugation quantum number). The exotic amplitude U_1 is therefore expected to be small and to decrease rapidly at high energies. We can thus assume that

$$U_1 = 0 \text{ for } k_{1\mathrm{ab}} \gtrsim 4 \text{ GeV}. \tag{19}$$

This assumption implies the equalities

$$P = T = P_N \text{ and } H_1 = H_1' = N_1. \tag{20}$$

The present data at 4 GeV are consistent with this conclusion (Fig. 6).

The exotic character of the amplitude U_1 means that $\bar{\alpha}_1 < 0$ so that U_1 is, in fact, a superconvergent amplitude. $\mathrm{Im}U_1$ is large at low energies and $Q_1^{(U)}$ and $\mathrm{Im}U_1$ at the cutoff energy have the same signs (Figs. 1 and 4). The one-effective-pole approximation of $\mathrm{Im}U_1$ is therefore clearly inadequate. A secondary term that is large at low energies but vanishes fast with increasing energy is needed. This problem has been recognized also by Barker *et al.*[15] who add two additional terms to account for the behavior of U_1. Importantly, they find the effect of U_1 small and consistent with $U_1 = 0$ for $k_{1\mathrm{ab}} \gtrsim 4$ GeV.

With $U_1 = 0$, Eqs. (5) reduce to a simple quadratic equation for the amplitude U_0 which is dominated by B exchange and/or ρP Regge cuts. For $t \lesssim -0.9$ this equation has only complex solutions for both low-energy inputs and all considered $\bar{\alpha}_0$. Because acceptable changes in the input σ_U do not yield real solutions, we have decreased the magnitude of $Q_0^{(U)}$ to obtain a zero radical and a real solution for $\mathrm{Im}U_0$. (The largest decrease of $Q_0^{(U)}$ is 5% at $t=-0.8$ GeV^2 and 30% at $t=-1.1$ GeV^2.)

The two solutions for $\mathrm{Im}U_0$ have a t structure essentially insensitive to the low-energy input and variations of $\bar{\alpha}_0$. One solution is negative and its magnitude decreases with increasing $-t$. For $\bar{\alpha}_0 < 0$ it changes sign and the zero moves to $t \approx -0.9$ GeV^2 for decreasing values of $\bar{\alpha}_0 < 0$. This behavior is in accord with the analysis[13] and solution I of Ref. 34. The second solution is positive and changes sign for $|t| \approx 0.6$–0.8 GeV^2, in accord with the analysis.[14] It is also qualitatively similar to $\mathrm{Im}U_0$ of Ref. 15 and solution II of Ref. 34 which, however, show a change of sign at $t \approx -0.4$ and $t \approx -0.2$ GeV^2, respectively.

In the absence of data on polarization parameters that measure the interference of U_0 with large and better known amplitudes N_1 or N_0, the two solutions are, in general, both acceptable since the existing data do not discriminate well between them. The information on recoil-nucleon polari-

zation P is not very useful in this respect because, together with T, it measures the interference of U_0 with a small amplitude U_1, and the errors are large.

Although the error bars on σ_U are rather large, better fits to σ_U at higher energies are obtained with $\bar{\alpha}_0$ higher than the typical α_B Regge trajectory[32]

$$\alpha_B = -0.02 + 0.7t$$

(t in GeV^2) and, in fact, for $\bar{\alpha}_0 > 0$. Consequently, we have further simplified our analysis with an additional assumption that

$$\bar{\alpha}_0 = \alpha_0 . \tag{21}$$

We have found no value of $\bar{\alpha}_0$ for which the positive root for $\mathrm{Im}U_0$ gives acceptable fit to σ_U for $t \approx 0.6$–0.7 GeV^2 for either low-energy input. We therefore present in Secs. V–VII the results corresponding to the negative root of $\mathrm{Im}U_0$ (solution I), but comment on the solution with the positive root of $\mathrm{Im}U_0$ (solution II) in Sec. VII. As we shall see, it is this particular choice of solution for $\mathrm{Im}U_0$ (<0) that is fully responsible for the zero structure of $\mathrm{Im}H_0$ at $t \approx -0.2$ GeV^2.

V. ANALYSIS WITH ONE LINEAR EFFECTIVE TRAJECTORY

The experimental effective trajectory of $\gamma p \to \pi^0 p$ is shown in Fig. 7. It can be described by a linear fit[33]

$$\alpha = 0.2 + t/3 , \tag{22}$$

(t in GeV^2). With the assumption that

$$\alpha_0 = \alpha_1 = \alpha , \tag{23}$$

the effective trajectory (22) was used in the original amplitude analysis[13] together with the older pion photoproduction multipole analysis of Walker.[22] To examine the sensitivity of this amplitude analysis to the low-energy input, we have repeated the calculations with the newer low-energy solutions of Metcalf and Walker[28] and Moorehouse *et al.*[25]

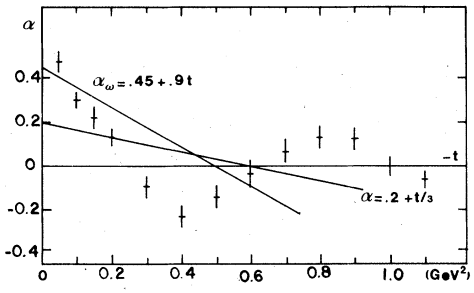

FIG. 7. The experimental effective trajectory in $\gamma p \to \pi^0 p$ (Ref. 33).

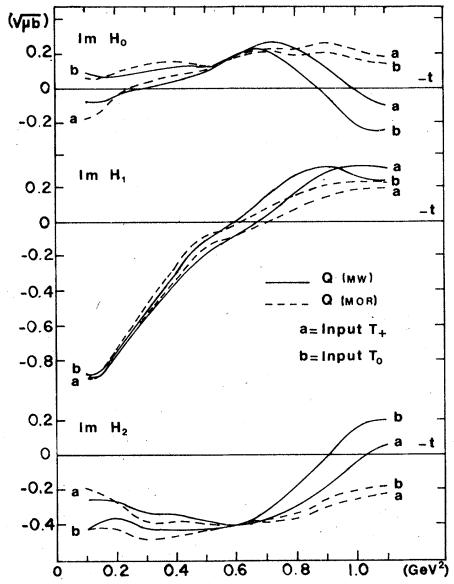

FIG. 8. The solution for $\mathrm{Im}H_n$ with the linear effective trajectory (22).

With the assumption (23) we have a quadratic equation for $\mathrm{Im}N_1$. For Q(MW) and T_0 and T_- we encounter complex solutions for $|t| \gtrsim 0.8$ and the magnitude of the input target asymmetry was reduced to obtain a zero radical and real solutions. The solution for natural amplitudes is determined unambiguously when we require (a) $\mathrm{Im}N_1 < 0$ for $|t| < 0.5$ and $\mathrm{Im}N_1 > 0$ for $|t| > 0.7$ GeV^2, (b) continuity and smoothness of $\mathrm{Im}N_1$ as a function of t. The negative solution for $\mathrm{Im}U_0$ was used to reconstruct the amplitudes H_0 and H_2. We recall that

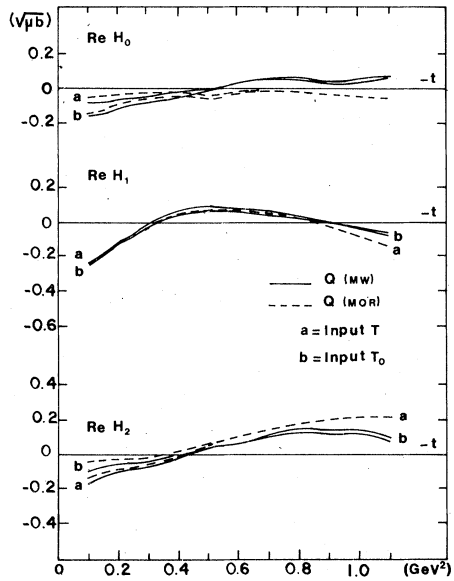

FIG. 9. The solutions for $\mathrm{Re}H_n$ with linear effective trajectory (22).

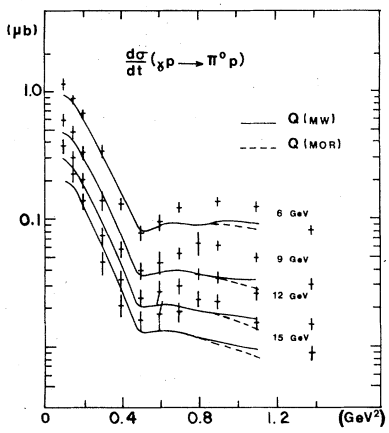

FIG. 10. Predictions for $d\sigma/dt$ from the solutions with the linear effective trajectory (22) and T_+ input for the polarized-target aymmetry. Data from Ref. 6.

$H_1 = N_1$.

The results for $\mathrm{Im}H_n$, $n = 0, 1, 2$, are shown in Fig. 8 for T_+ and T_0 inputs. The corresponding real parts are shown in Fig. 9. We comment on the results with T_- polarization input in Sec. VIII.

We first notice that the t structure of $\mathrm{Im}H_0$ for $|t| \lesssim 0.3$ GeV^2 is very sensitive to the input target asymmetry and only with T_+ do we obtain the typical J_0 zero at $-t \approx 0.2$–0.3 GeV^2. $\mathrm{Im}H_1$ exhibits J_1 t structure for all input variations. The only feature significantly dependent on the low-energy input is the behavior of $\mathrm{Im}H_0$ and $\mathrm{Im}H_2$ for $-t \gtrsim 0.9$ GeV^2—there is no change of sign for Q(MOR) input independently of the target-asymmetry input. However, the decreasing magnitudes of $\mathrm{Im}H_2$ for Q(MOR) indicates a possible zero at larger values of t.

The t structure of $\mathrm{Re}H_n$, $n = 0, 1, 2$, is essentially insensitive to the input polarization. The differences in $\mathrm{Re}H_0$ and $\mathrm{Re}H_2$ for the two low-energy inputs reflect similar differences for $\mathrm{Im}H_0$ and $\mathrm{Im}H_2$ for $-t \gtrsim 0.9$ GeV^2. $\mathrm{Re}H_1$ has two zeros, at $t \approx -0.3$ and $t \approx -0.9$ GeV^2, independently of the low-energy and polarization input.

The predictions for $d\sigma/dt$ at higher energies are shown in Fig. 10 for the T_+ input. The results with T_0 and T_- inputs are very similar. We notice that predictions at $t \approx -0.1$ and $t \lesssim -0.7$ GeV^2 are not very satisfactory. We attempted to improve these results by considering also other linear trajectories, including $\alpha_\omega = 0.45 + 0.9t$ (t in GeV^2). We found that while the t structure of amplitudes is not sensitive to such variations of α, the desired overall improvement in the energy dependence of $d\sigma/dt$ was not achieved. Consequently, as in πN CEX,[18] we have attempted a modified analysis involving effective Regge trajectories.

VI. ANALYSIS WITH INDEPENDENT EFFECTIVE TRAJECTORIES (ERPA)

For each low-energy and polarization input, we searched in this analysis, t by t, for values of α_0 and α_1 that produce solutions with the following properties:

$$\begin{aligned} &\text{(i) } \mathrm{Im}H_1 < 0 \text{ for } |t| \lesssim 0.5 \text{ GeV}^2, \\ &\quad \mathrm{Im}H_1 > 0 \text{ for } |t| \gtrsim 0.8 \text{ GeV}^2 \text{ (see Fig. 3).} \end{aligned} \tag{24}$$

(ii) The values of $d\sigma/dt$ and photon asymmetry A calculated at higher energies are within the error bars of the data.

(iii) The amplitudes are continuous and smooth functions of t.

Throughout this search the values of α_0 and α_1 were independent and within the range

$$\begin{aligned} &0.45 + 1.8t \lesssim \alpha_n \lesssim 0.45 \text{ for } |t| \lesssim 0.4 \text{ GeV}^2, \\ &-0.25 \lesssim \alpha_n \lesssim 0.45 \text{ for } |t| > 0.4 \text{ GeV}^2. \end{aligned} \tag{25}$$

For $|t| \lesssim 0.4$ GeV^2 somewhat higher values of α_0 ($\alpha_0 \lesssim 0.6$) were also considered.

In addition to obtaining better fits to $d\sigma/dt$ and α at higher energies, the purpose of this study was to examine also the questions of uniqueness of the solutions and the stability of their t structure. We comment on these aspects before we present our results.

The answer to the first question is a conditional yes. At a given value of t there are, in general, more than one acceptable solution and some bias is necessary to single out a unique overall solution.

Because $\alpha_0 \neq \alpha_1$, the equation for $\mathrm{Im}N_1$ is a biquadratic equation. Although for some values α_0 and α_1 there are no real solutions, in general there are two complex and two real solutions for $\mathrm{Im}N_1$. The physically interesting solution can be selected unambiguously. For $-t \lesssim 0.5$ GeV^2 the two solutions have opposite signs. For $-t > 0.5$ GeV^2 we choose the solution smoother in t (the rejected solution is, in fact, the continuation of the solution for $\mathrm{Im}N_1$ which is positive for $-t < 0.5$ GeV^2).

Serious sources of double ambiguity are therefore only the two solutions for $\mathrm{Im}U_0$. We refer to solutions for SHA corresponding to the negative and positive roots for $\mathrm{Im}U_0$ as solution I and solution II, respectively. Solution II was rejected because for all considered values of α_0 and α_1 the predictions for σ_U and A at higher energies were unsatisfactory for $0.6 \lesssim |t| \lesssim 0.7$ GeV^2. This difficulty can be traced to the zero of $\mathrm{Im}U_0$ in this region of t. We further comment on solution II in Sec. VIII.

The requirements of smooth behavior of ampli-

tudes and goodness of the fit in the variable t thus lead to a unique overall solution.

The answer to the second question is affirmative. Both the accepted and rejected solutions for $\mathrm{Im}H_n$, $n=0, 1, 2$, have a t structure stable against variations of effective trajectories, even for values of α_0 and α_1 which produce less satisfactory fits to the data above 4 GeV. The real parts $\mathrm{Re}H_n$ have a t structure more sensitive to such changes but their t structure is very similar and stable for values α_0 and α_1 which produce physical solutions satisfying the requirements (24).

We now present solution I for T_+ and T_0 input target asymmetry. We also briefly comment on the results with the T_- input.

Because the data on $d\sigma/dt$ and A extend to only 15 and 10 GeV, respectively, the determination of the values of α_0 and α_1 is not as restrictive as in πN CEX.[18] We have thus determined (at each value of t and for each input) the ranges I_0 and I_1 of values α_0 and α_1 that give an acceptable solution. These are shown in Fig. 11. The values of α_0 and α_1 are, however, correlated so that not every pair of α_0 and α_1 from I_0 and I_1 gives an acceptable solution. The correlations between α_0 and α_1 are illustrated in Fig. 12 for the T_+ input at $t=-0.1$, -0.4, -0.6, and -1.1 GeV^2.

The solutions for U_0 and N_0 are shown in Figs. 13 and 14. Those for $\mathrm{Im}H_n$, $n=0, 1, 2$ are shown in Fig. 15. The corresponding real parts are shown in Fig. 16. In Fig. 17 we show the fits to

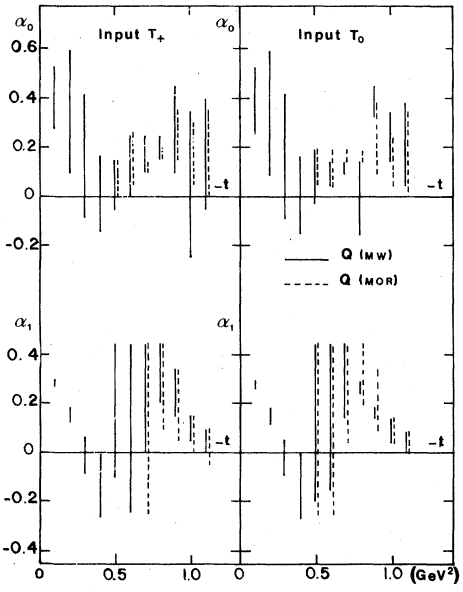

FIG. 11. Final values of the effective trajectories α_0 and α_1 for T_+ and T_0 polarization inputs. The dashed lines show α_0 and α_1 for the Q(MOR) input where they do not coincide with those for the Q(MW) input.

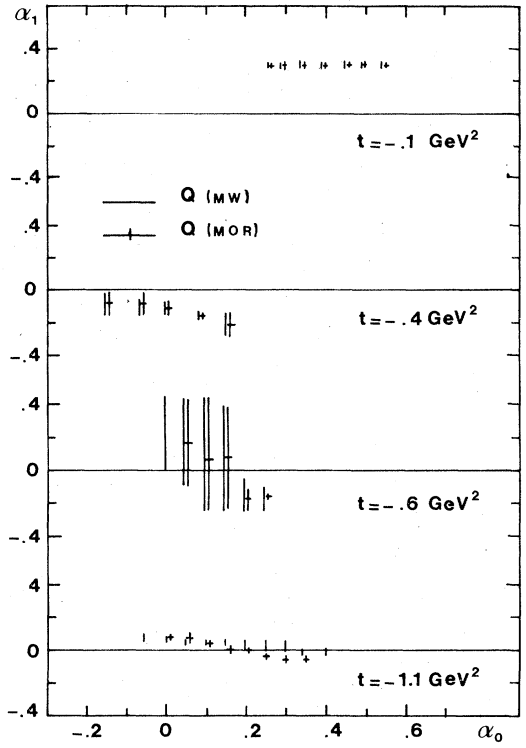

FIG. 12. Correlations between α_0 and α_1 for the polarized-target asymmetry input T_+.

$d\sigma/dt$ for the solution with T_+ and Q(MW) input. The results for other inputs are virtually identical.

$\mathrm{Im}U_0$ has no zero structure but $\mathrm{Re}U_0$ changes sign at $t\approx-0.5$ GeV^2. The magnitude of $\mathrm{Im}N_0$ is very sensitive on the polarization input for $|t| \lesssim 0.3$ GeV^2. $\mathrm{Im}N_0$ changes sign at $t\approx-0.9$ GeV^2 for the Q(MW) input but there is no change of sign for the Q(MOR) input. This is the only appreciable difference between the two low-energy inputs in our analysis. It is due to large values of Q_0 and

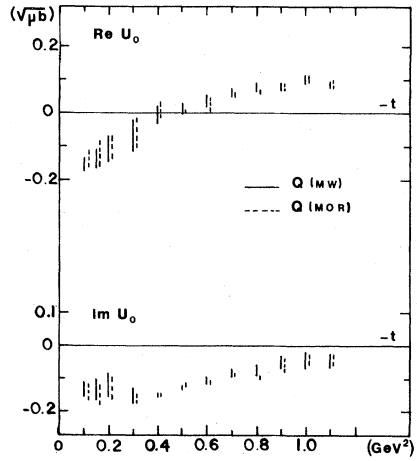

FIG. 13. The solution I for the unnatural amplitude U_0.

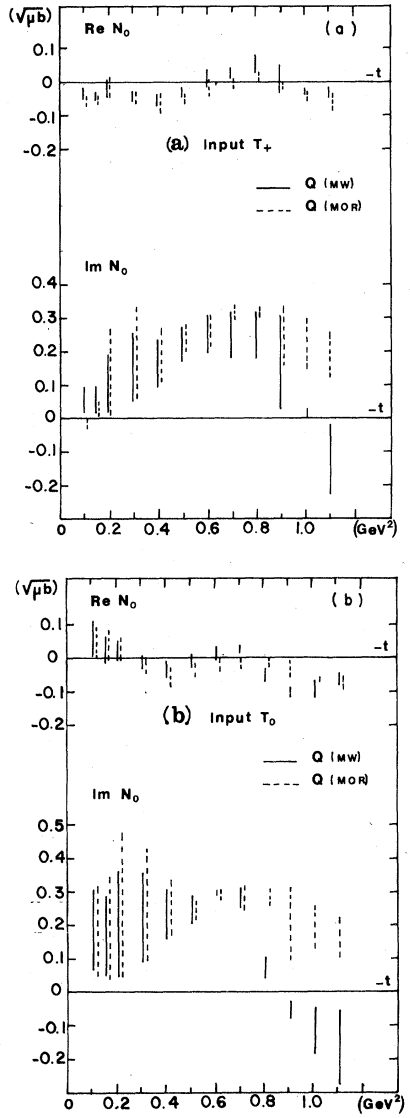

FIG. 14. The solution for the natural amplitude N_0 and its dependence on polarized-target asymmetry: (a) input T_+ (b) input T_0.

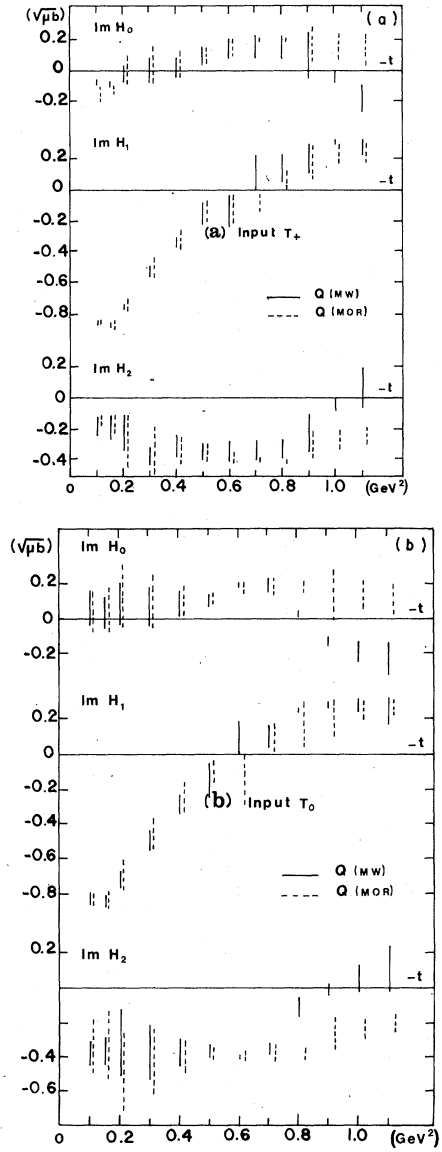

FIG. 15. The solution for imaginary parts $\mathrm{Im}H_n$ and their dependence on polarized-target asymmetry: (a) input T_+ (b) input T_0.

Q_2 in the Q(MOR) input. However, these are subject to a modification by contributions from higher-mass resonances above 1.2 GeV (Ref. 25) so that the result with Q(MW) is more likely correct. $\mathrm{Re}N_0$ shows a clear tendency for a double-zero structure in the range $-t \approx 0.5$–0.9 GeV^2 but the position of zeros is not conclusive.

$\mathrm{Im}H_0$ is sensitive to the input target asymmetry for $|t| \lesssim 0.3$ GeV^2. Its zero at $-t \approx 0.2$–0.3 GeV^2 is a direct consequence of the choice of the negative solution for $\mathrm{Im}U_0$, but for T_- input $\mathrm{Im}H_0$ is positive and large at these values of t. The peripheral J_0 structure is thus clear only for the T_+ polarization input. As the value of the polarization T decreases, the peripheral structure of $\mathrm{Im}H_0$ disappears.

$\mathrm{Im}H_1$ exhibits a clear J_1 t structure with a zero at $-t \approx 0.6$–0.7 GeV^2 and is remarkably stable against changes in the low-energy and polarization inputs. $\mathrm{Im}H_2$ shows a peripheral J_2 structure for the Q(MW) which is not observed for the Q(MOR) input. Again, this difference for $-t \gtrsim 0.9$ GeV^2 is the only appreciable divergence between the results from the two low-energy inputs.

$\mathrm{Re}H_1$ does not have the typical simple Regge-pole double zero at $t \approx -0.6$ GeV^2. It has a zero at $t \approx -0.3$ GeV^2 and a possible zero at $-t \approx 1.0$–1.1 GeV^2. The zero at $t \approx -0.3$ GeV^2 is independent of the input T, including the input T_-. $\mathrm{Re}H_2$ vanishes

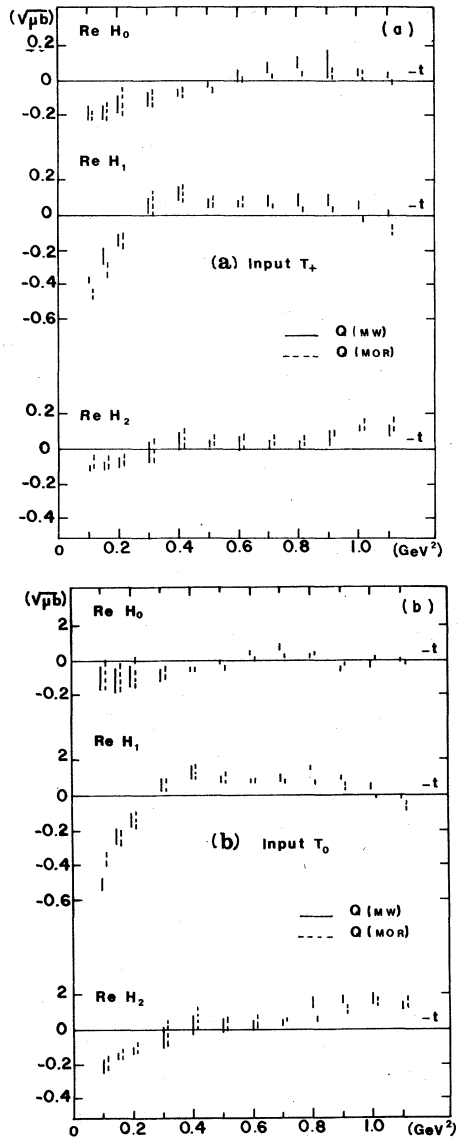

FIG. 16. The solution for real parts $\mathrm{Re}H_n$ and their dependence on polarized-target asymmetry: (a) input T_+ (b) input T_0.

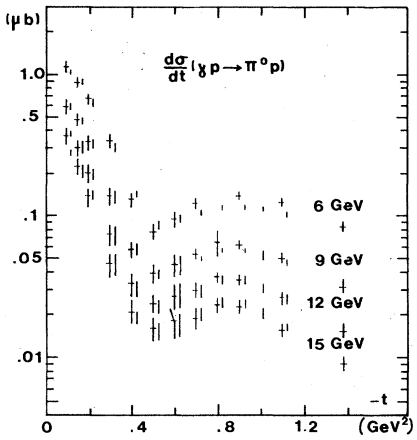

FIG. 17. Fits to $d\sigma/dt$ of the solution with the input T_+ and Q(MW), and the effective trajectories of Fig. 11. Data from Ref. 6.

also at $t \approx -0.3$ GeV^2 but $\mathrm{Re}H_0$ has a zero at $t \approx -0.55$ GeV^2.

The energy dependence of the amplitudes deviates considerably from the conventional α_ω and $\alpha_{\omega\rho}$ linear Regge trajectories. For $-t \lesssim 0.5$ GeV^2 the trajectory α_0 is consistent with $\alpha_\omega = 0.45 + 0.9t$ (t in GeV^2) but α_1 is not. In this respect the single-flip amplitude in $\gamma p \to \pi^0 p$ differs from the πN CEX single-flip amplitude.[18] The difference in the energy dependence is also reflected in the different behavior of $\mathrm{Re}H_1$.

We also note that the resulting effective trajectories α_0 and α_1, in particular their t structures, are not very sensitive to the low-energy and polarization inputs. This observation suggests that α_0 and α_1 may well approximate the true energy dependence of the amplitudes.

The results of the analysis with the T_- input are very similar to those with T_+ and T_0 inputs except for the nonflip amplitude. $\mathrm{Im}H_0$ is positive and relatively large for $-t \lesssim 0.4$ GeV^2. It changes sign at $-t \approx 0.7$–0.8 GeV^2 for the Q(MW) input. For the Q(MOR) there is no change of sign although $\mathrm{Im}H_0$ dips at $t \approx -0.5$ GeV^2. $\mathrm{Re}H_0$ is positive for $-t \lesssim 0.2$ GeV^2 and its clear single-zero structure at $t \approx -0.55$ GeV^2 for T_+ and T_- develops into a double-zero structure with zeros at $t \approx -0.2$ and $t \approx -0.45$ GeV^2. It is interesting that $\mathrm{Re}H_1$ retains its zero at $t \approx -0.3$ GeV^2.

Present data on nucleon polarization P and photon asymmetry A eliminate this solution because the inequality[3] $|T - P| \leq 1 - A$ is violated for T_- at $t \approx -0.2$ GeV^2. However, for $-t \gtrsim 0.3$ GeV^2 this solution is still acceptable.

VII. PREDICTIONS FOR POLARIZATION PARAMETERS

In our analysis some perfect fits to $d\sigma/dt$ were rejected because the predictions for photon symmetry A at 6 and 10 GeV were not acceptable. We expect that other polarization parameters measured at $P_{\mathrm{lab}} \approx 4$ GeV or higher energies will have additional discriminatory power useful in this type of amplitude analysis.

The single-polarization parameters were defined in Eqs. (1b)–(1d). Figure 18 shows fits and predictions for photon asymmetry at 6, 10, and 15 GeV. The predictions for target asymmetry at 15 GeV are shown in Fig. 19. We recall that $P = T$ in our analysis.

For double-polarization parameters we have used those defined by Barker, Donnachie, and

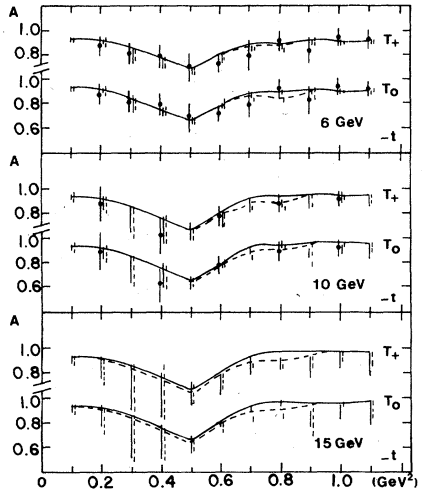

FIG. 18. Fits and predictions for the polarized-photon asymmetry A from solutions with the linear effective trajectory (22) (solid and dashed curves) and the effective trajectories of Fig. 11 (solid and dashed vertical lines). Data from Ref. 6.

Storrow (BDS) in Ref. 4. The three sets of four double-polarization parameters reduce to one set of four and one set of three, following our assumption that $U_1 = 0$.

With our notation for the $\gamma p \to \pi^0 p$ amplitudes (1) and $U_1 = 0$, the BDS double-polarization parameters can be written as follows:

Beam-target:

$$
\begin{aligned}
G\frac{d\sigma}{dt} &= -2\,\mathrm{Im}(H_0 H_2^*) = +4\,\mathrm{Im}(N_0 U_0^*), \\
H\frac{d\sigma}{dt} &= -2\,\mathrm{Im}[H_1(H_0 + H_1)^*] = -4\,\mathrm{Im}(N_1 U_0^*), \\
E\frac{d\sigma}{dt} &= |H_0|^2 - |H_2|^2 = +4\,\mathrm{Re}(N_0 U_0^*), \\
F\frac{d\sigma}{dt} &= +2\,\mathrm{Re}[H_1(H_0 + H_2)^*] = +4\,\mathrm{Re}(N_1 U_0^*).
\end{aligned}
\tag{26}
$$

Beam-recoil:

$$
O_x = H, \quad O_z = G, \quad C_x = F, \quad C_z = E. \tag{27}
$$

Target-recoil:

$$
\begin{aligned}
T_x\frac{d\sigma}{dt} &= 2|H_1|^2 + 2\,\mathrm{Re}(H_0 H_2^*) \\
&= 2(|N_1|^2 - |N_0|^2 + |U_0|^2), \\
T_z\frac{d\sigma}{dt} &= 2\,\mathrm{Re}[H_1(H_0 - H_2)^*] = +4\,\mathrm{Re}(N_0 N_1^*), \\
L_x &= T_z, \\
L_z\frac{d\sigma}{dt} &= 2|H_1|^2 - |H_0|^2 - |H_2|^2 \\
&= 2(|N_1|^2 - |N_0|^2 - |U_0|^2).
\end{aligned}
\tag{28}
$$

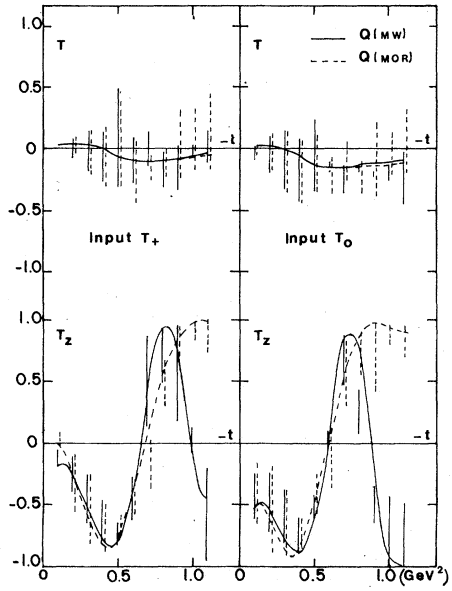

FIG. 19. Predictions for the polarized asymmetry T and the parameter T_z at 15 GeV. Description as in Fig. 18.

The interference between the amplitudes N_0 and N_1 is measured by the polarized-target asymmetry T and the parameter T_z. Figure 19 shows the predictions of our analysis with linear and effective trajectories (Secs. V and VI) at 15 GeV. The positive values of T at $t = -0.5$ GeV^2 correspond to $\alpha_0 \lesssim 0.05$ and $\alpha_1 \gtrsim 0.15$. The predictions for T_z at 4 GeV are similar to those at 15 GeV.

The interference of the amplitude U_0 with N_0 and N_1 is measured by the double-polarization

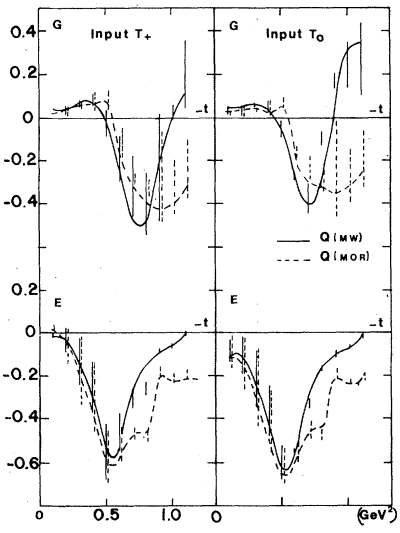

FIG. 20. Predictions for the double-polarization parameters G and E at 4 GeV. Description as in Fig. 18.

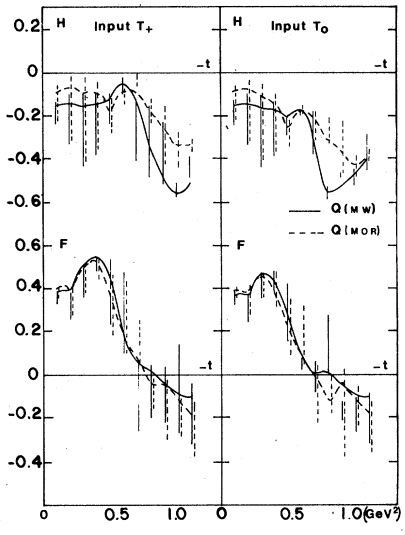

FIG. 21. Predictions for the double-polarization parameters H and F at 4 GeV. Description as in Fig. 18.

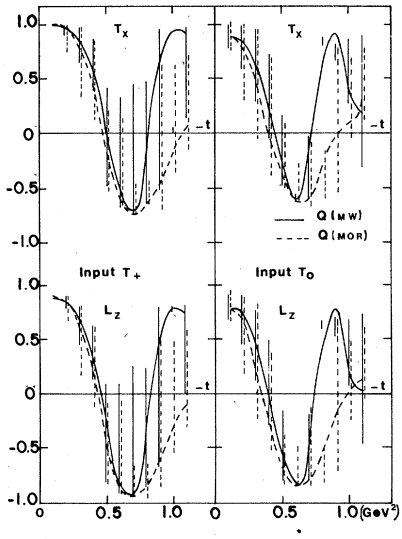

FIG. 22. Predictions for the double-polarization parameters T_X and L_Z at 4 GeV. Description as in Fig. 18.

parameters G, E and H, F, respectively. The predictions at 4 GeV for these two pairs of parameters are shown in Figs. 20 and 21. The predictions at 4 GeV for the parameters T_X and L_Z are presented in Fig. 22. The energy dependence of all these parameters is rather weak, and at 15 GeV their behavior is similar to that at 4 GeV for all input variations.

VIII. DISCUSSION

A. The solution II and possible ambiguity in π° photoproduction analyses

The solutions I and II have a common single-flip amplitude $H_1 = N_1$. Also, the amplitudes H_0 and H_2 are common for $-t \gtrsim 0.9$ GeV^2. For $-t < 0.9$ GeV^2, their differences are defined by the two different solutions for ImU_0. In solution II, ImU_0 is positive and changes sign for $-t \approx 0.6$–0.8 GeV^2 in contrast to the negative and structureless ImU_0 in solution I.

For $-t \lesssim 0.5$ GeV^2, ImH_0 and ImH_2 of solution II differ considerably from those of solution I. For all considered low-energy and polarization inputs, ImH_0 is positive and its magnitude increases with decreasing values of the input T. ImH_2 is very sensitive on the polarization input for $-t \lesssim 0.4$ GeV^2. For the input T_+, ImH_2 is positive at $t \approx -0.1$ GeV^2 and changes sign at $-t \approx 0.2$–0.3 GeV^2. For T_0 it is very small and its sign is not certain for $-t \lesssim 0.3$ GeV^2. For T_- ImH_2 is definitely negative. Both ImH_0 and ImH_2 change signs at $t \approx -0.85$ GeV^2 for Q(MW) input, but there is no such change for the Q(MOR) input.

ReH_0 is positive and changes sign at $t \approx -0.6$ GeV^2 for T_+ and $t \approx -0.85$ GeV^2 for T_0 inputs. ReH_2 is structureless flat positive function for the T_+ input. ReH_2 is somewhat sensitive on the polarization input for $-t \lesssim 0.3$ GeV^2. For the T_- input it is negative and changes sign at $t \approx -0.2$ GeV^2.

Solution II is consistent with the amplitudes obtained by Barbour and Moorhouse[14] and by Barker, Donnachie, and Storrow.[15] In the latter analysis, however, ImH_0 has the zero at $t \approx -0.6$ GeV^2. To a lesser extent, this solution is also consistent with the behavior of amplitudes at $k_{1\,\mathrm{ab}} = 1.7$ GeV in the low-energy analysis of Metcalf and Walker (see Fig. 5) and solution II of Goldstein *et al.*[34] (except for their ReH_1). In these two analyses, ImH_0 has the zero at $t \approx -0.3$ and $t \approx -0.2$ GeV^2, respectively.

Solution II does not fit well with the photon asymmetry A for $-t \approx 0.6$–0.8 GeV^2 at 6 and 10 GeV and the closes analysis of Barbour and Moorhouse[14] suffers from the same difficulty. The reason is the zero structure of ImU_0 in this t region. Because solution I does fit the photon asymmetry, and because its ImH_0 is peripheral for the very likely correct values of the input target asymmetry, we have rejected solution II in our analysis.

This bias in the selection of solution could be, of course, criticized. For instance, it could be argued that an incorporation of the amplitude U_1 could remedy the difficulty of solution II. Indeed, the equality $T = P$ seems to be least satisfied for $-t \gtrsim 0.5$ GeV^2 (Fig. 6), and Barker *et al.*,[15] who in their analysis do not neglect the amplitude U_1, do fit the photon asymmetry A at $t = -0.6$ GeV^2. However, their analysis does not extend to larger

values of t.

We therefore conclude that we may be faced with an inherent double ambiguity in amplitudes H_0 and H_2 in our analysis. This ambiguity may be removed only by a measurement of at least one of the four beam-target double-polarization parameters which measure the interference of the amplitude U_0 with the amplitudes N_0 and N_1. Irrespective of the input, the predictions of the two solutions are relatively large and of opposite sign for $0.3 \lesssim -t \lesssim 0.6$ for G and E, and for $0.1 \lesssim -t \lesssim 0.5$ for H and F. It may be of interest that the predictions for the parameters G and H of our solution II are in agreement with those of Barker *et al.*[15] for $-t \lesssim 0.5$ GeV^2.

B. Polarization and the t structure of amplitudes

An important conclusion of our analysis is that the zero structure of $\mathrm{Re}H_1$ and $\mathrm{Im}H_1$ is independent of the polarization structure. $\mathrm{Re}H_1$ maintains its zero at $t \approx -0.3$ GeV^2 also for the T_- input and thus cannot be responsible for the zero of T_+ and T_0 as it is usually assumed.[14] The zero of T_+ and T_0 comes from cancellations of the interfering terms and is rather associated with the t structure of $\mathrm{Im}H_0$ in solution I (or $\mathrm{Im}H_2$ in solution II). The peripheral structure of $\mathrm{Im}H_0$ in our solution I is seen only for positive and sufficiently large T for $-t \lesssim 0.3$ GeV^2. There does not appear to be any feature of the polarization T which would necessarily require peripheral J_2 structure of $\mathrm{Im}H_2$, as is evidenced by our results with the Q(MOR) input. This large t structure appears to be more sensitive on the low-energy contribution of the FTDR to the real parts. Also, for all inputs $\mathrm{Re}H_0$ and $\mathrm{Re}H_2$ maintain their zeros at $t \approx -0.5$ and $t \approx -0.3$ GeV^2, respectively.

C. Implications of the stability of solutions

An important conclusion of our analysis is the stability of the t structure of solutions for $\mathrm{Im}H_n$ against large variations of input effective trajectories. In particular, the zeros of $\mathrm{Im}H_n$ are not associated with any particular value of α_n. $\mathrm{Re}H_n$ are more sensitive to such variations but their t structure is remarkably stable for those values of input α_n which provide good fits to $d\sigma/dt$ at higher energies.

This stability suggests that even if we commit some error in the treatment of energy dependence of amplitudes, their t structure is likely to remain unchanged. It also suggests that the mechanisms responsible for the t structure and s dependence of $\mathrm{Im}H_n$ are not strongly interrelated. This conclusion is consistent with the spirit of the dual absorptive model[35] which specifies the t structure of $\mathrm{Im}H_n$, but leaves the question of their energy dependence open. On the other hand, it contradicts certain models in which the t structure of amplitudes is tied to the assumptions about energy dependence (e.g., simple Regge-pole model with nonsense wrong-signature zero and weak Regge-cut models).

D. The structure of real parts of amplitudes and finite-energy sum rules

Although the parametrization (11) of imaginary parts is assumed to be a good approximation at finite energies, FTDR's introduce terms into the real parts which are important contributions at finite energies. Only in the limit $\nu \to +\infty$ is the whole amplitude dominated by the simple Regge-pole form. At finite energies the FTDR corrections are essential for an explanation of the t structure of real parts and polarization data.

We can write Eq. (13) in the form

$$\mathrm{Re}H_n(\nu,t) = \tan\left(\frac{\pi}{2}\alpha_n\right)\mathrm{Im}H_n(\nu,t) + C_n(\nu,t), \quad (29)$$

where

$$C_n(\nu,t) = \frac{1}{\nu^2}\left[Q_n(t) + \frac{2}{\pi}\frac{N^{1+\alpha_n}}{1+\alpha_n}\beta_n(t)\right]. \quad (30)$$

The deviations of $\mathrm{Re}H_n$ from a simple Regge structure are understood in our approach in terms of deviations from finite-energy sum rules (FESR) for the effective Regge-pole approximation of $\mathrm{Im}H_n$. The origin of the FTDR corrections to real parts is therefore in the nonperipheral character of contributions from certain low-energy resonances and the unphysical region to the dispersion integral.

We have verified explicitly in $\gamma p \to \pi^0 p$ that when nucleon and $P_{33}(1236)$ contributions are subtracted from the (low-energy) FESR moments $Q_n^{(k)}$, $k = 0, 1, 2, 3$, the resulting $\tilde{Q}_n^{(k)}$ have a more peripheral t structure already for $k = 0$ and reproduce well the t structure of $\mathrm{Im}H_n$ at the cutoff energy for the higher moments. Higher-order FESR's for $k \geq 1$ are, however, well satisfied even without such subtraction.[13] Armenian *et al.*[48] obtain a similar result in their analysis based on semilocal duality.

We now comment on another aspect of the nonperipheral contributions to FTDR's. We can write (for $k = 0$)

$$Q_n(t) = K_n(t) + P_n(t), \quad (31)$$

where K_n and P_n are nonperipheral and peripheral contributions to Q_n, respectively. Since the nonperipheral contributions are associated with low values of angular momentum and are rather strong

in certain amplitudes, it is not surprising that they give large contributions for small values of b in the impact-parameter representation of $\mathrm{Re}H_n$. On the other hand, large contributions near $b \approx 0$ are usually associated with amplitudes in elastic scattering (e.g., Ref. 36). Jakob has shown[37] that the relation between nonperipheral contributions K_n and elastic scattering is provided in πN CEX by unitarity.

E. Absorption effects and comparison with Regge-cut models

It is useful to define pragmatically the absorption or Regge-cut contributions as the difference between the features of amplitudes required by data and those given by the simple Regge-pole model (with nonsense wrong-signature zeros[38]).

The J_1 structure of $\mathrm{Im}H_1$ is consistent with no or small absorption effects in $\mathrm{Im}H_1$. $\mathrm{Re}H_1$ in $\gamma p \to \pi^0 p$ is considerably more absorbed than $\mathrm{Re}H_1$ in πN CEX as evidenced by its zeros at $t \approx -0.3$ and -1.1 GeV^2. We can infer this also from the much larger deviations of α_1 from a linear trajectory for $-t \gtrsim 0.2$ GeV^2 as contrasted with smaller deviations of α_1 from α_ρ for $-t \lesssim 0.6$ GeV^2 in πN CEX.[18] These differences may be related to a possible dependence of absorptive corrections on external masses,[39-41] or different forms of t-channel unitarity for photoproduction and purely hadronic reactions.[41]

In $\gamma p \to \pi^0 p$, a simple Regge pole and the weak-cut model[42] predict for $\mathrm{Re}H_1$ a double-zero structure at $t \approx -0.5$ GeV^2 and they both make the wrong prediction for the polarized-target asymmetry T. The models with stronger cuts[43-45] give $\mathrm{Re}H_1$ with a t structure similar to our results but they also fail in their prediction for T. On the other hand, the eikonal model[46] does fit T but has $\mathrm{Re}H_1$ that does not change sign but dips at $t \approx -0.65$ GeV^2. Since the t structure of $\mathrm{Re}H_1$ in both πN CEX and $\gamma p \to \pi^0 p$ does not depend on the input polarization (or on the choice of solution for U_0 in $\gamma p \to \pi^0 p$), we may conclude that the present Regge-cut models need some modifications.

As in πN CEX,[18,47] the nonflip amplitude is the most sensitive amplitude on the input polarization. This is particularly true for the exact position of zero of $\mathrm{Im}H_0$ and the details of the t structure of $\mathrm{Re}H_0$. The insensitivity on the input T of the zero of $\mathrm{Re}H_0$ at $t \approx -0.5$ GeV^2 contrasts with πN CEX where, at 6 GeV, the zero structure of $\mathrm{Re}H_0$ depends very much on the polarization input.[18,47] The zero structure of $\mathrm{Re}H_0$ in $\gamma p \to \pi^0 p$ contradicts all Regge-cut models (e.g., Refs. 42 and 46 have no zero; Refs. 45 and 44 have a zero at $t \approx -0.2$ GeV^2). Our analysis suggests that $\mathrm{Re}H_0$ is less absorbed than $\mathrm{Im}H_0$ at 4–6 GeV, but the absorption tends to increase with energy. This simply reflects the diminishing effect of the low-energy contributions to the dispersion integral.

Although the position of zero of $\mathrm{Im}H_2$ is sensitive to the large discrepancies in the low-energy input, the overall behavior of $\mathrm{Im}H_2$ suggests that it is more absorbed than $\mathrm{Re}H_2$ which has a zero at $t \approx -0.3$ GeV^2 independently of the polarization input (including T_-). This structure of $\mathrm{Re}H_2$ is closer to that of Ref. 43 than that of Ref. 46 who obtained zero at $t \approx -0.7$ GeV^2. We must point out that for $\mathrm{Im}U_0 > 0$, the sensitivity of H_0 and H_2 on the input polarization is reversed.

Our results for effective trajectories confirm the generally accepted idea that absorption corrections are helicity-flip dependent. Their relations to absorption models are not clear. The large slope of α_1 for $-t \lesssim 0.4$ GeV^2 suggests a strong contribution from a term with a lower-lying trajectory (e.g., a Regge-Regge cut) but α_0 is very consistent with a linear α_ω trajectory. Both α_0 and α_1 indicate effects similar to Regge-Pomeron cuts for $-t \gtrsim 0.6$ GeV^2. The independence of the t structure of $\mathrm{Im}H_n$ on effective trajectories α_n is also not expected in absorption models.

We may conclude that there is a clear evidence for absorption effects in our solutions but that their manifestations in the zero structure of amplitudes and the behavior of α_n does not fully agree with any of the best studied models for absorption and Regge cuts.

IX. SUMMARY

We have used FTDR's and effective Regge-pole parametrization of imaginary parts of SHA's to transform the available high-energy data on $\gamma p \to \pi^0 p$ into direct information about the corresponding amplitudes. The reliability of this method was examined, to some extent, by studying the sensitivity of the solutions to the input data and large variations of effective trajectories. Our results may be summarized as follows:

(i) $\mathrm{Im}H_n$ have a peripheral t structure in both reactions. The peripheral behavior of $\mathrm{Im}H_0$ and $\mathrm{Im}H_2$ is due to the superposition of their natural and unnatural components, which by themselves are not peripheral.

(ii) Single-flip amplitude does not exhibit a simple Regge-pole–like behavior. $\mathrm{Re}H_1$ has zeros at $t \approx -0.3$ and $t \approx -1.1$ GeV^2. $\mathrm{Re}H_0$ resembles more a simple Regge pole. The zeros of $\mathrm{Re}H_0$ and $\mathrm{Re}H_2$ at $t \approx -0.5$ and $-t \approx 0.3$–0.5 GeV^2, respectively, are insensitive to polarization input.

(iii) The t structure of H_1 and H_2 is insensitive

to polarization input in contrast to H_0 which shows dependence on T for $-t \lesssim 0.4$ GeV^2. With decreasing values of T the peripheral character of ImH_0 disappears.

(iv) The discrepancies in the phase-shift analyses do not essentially influence the basic conclusions about the t structure and energy dependence of amplitudes. Their largest effect is on the zero structure of ImH_2 for $-t \gtrsim 0.9$ GeV^2.

(v) The t structure of ImH_n and ReH_1 is stable against large variations of the effective trajectories α_n indicating only a weak correlation between the t structure and energy dependence of amplitudes. This observation holds for all considered low-energy and polarization inputs.

(vi) Corrections to a simple Regge-pole exchange are indicated by both the t structure of SHA and the deviations of α_n from linear Regge trajectories. Our results confirm some general ideas about absorption effects but do not support any particular model. A comparison with πN CEX amplitudes suggests that a possible dependence of absorption on external masses seems to enter only in ReH_n and α_n since ImH_n have a similar t structure in both reactions.

(vii) In our solution II ImH_0 shows a nonperipheral behavior. The structure of ImH_2 is very sensitive on the input polarization. For the T_+ input polarization it has a zero at $-t \approx 0.2$–0.3 GeV^2. Although we rejected solution II, there is a possibility of a double ambiguity in π^0 photoproduction analyses which may be resolved only by a measurement of at least one double-polarization parameter at high energies.

Our analysis underlines a need for new experimental efforts in π^0 photoproduction. A measurement of the differential cross section and polarization parameters A, P, T over a broad range of energies and with improved statistics would enable a better determination of the energy dependence and t structure of amplitudes. Similar measurements in $\gamma n \to \pi^0 n$ would enable isotopic separation of exchange amplitudes. A measurement of at least one double polarization is extremely important to resolve a possible ambiguity in π^0 photoproduction amplitude analysis. Since π^0 photoproduction has always been important in shaping our ideas about hadron dynamics, such renewed experimental efforts are very well justified.

Note added. When this paper was completed we received a report by Barker and Storrow.[49] In their model they assume evasive Regge poles with nonsense wrong-signature zeros and self-conspiring structureless effective Regge cuts. Parameters are constrained by fits to FESR's using low-energy analysis of Moorhouse *et al.* They do not neglect the amplitude U_1 and obtain a good fit to A at higher energies. Their resulting amplitudes are virtually the same as amplitudes in our solution II with polarization input T_0 and low-energy input Q(MOR).

ACKNOWLEDGMENTS

The author wishes to thank Professor A. P. Contogouris and Professor V. Barger for stimulating discussions and Professor R. G. Moorhouse and Professor R. L. Walker for clarifying correspondence concerning their analyses of pion photoproduction. This work was supported in part by the National Research Council of Canada.

[1]W. Schmidt and G. Schwiderski, Fortschr. Phys. 15, 393 (1967).
[2]R. P. Worden, Nucl. Phys. B37, 253 (1977).
[3]G. R. Goldstein, J. F. Owens, J. P. Rutherford, and M. J. Morawczik, Nucl. Phys. B80, 164 (1974).
[4]I. S. Barker, A. Donnachie, and J. K. Storrow, Nucl. Phys. B95, 347 (1975).
[5]W. Braunschweig *et al.*, Phys. Lett. 26B, 405 (1968); Nucl. Phys. B20, 191 (1970).
[6]R. L. Anderson *et al.*, Phys. Rev. D 4, 1937 (1971).
[7]W. Braunschweig *et al.*, Nucl. Phys. B51, 167 (1973).
[8]P. S. L. Booth *et al.*, Phys. Lett. 38B, 339 (1972).
[9]H. Bienlein *et al.*, Phys Lett. 46B, 131 (1973).
[10]M. Deutsch *et al.*, Phys. Rev. Lett. 29, 1752 (1972).
[11]P. J. Bussey *et al.*, Experimental Proposal, Daresbury Laboratory, DL/SCP/108, 1975 (unpublished).
[12]M. Hontebeyrie, J. Procureur, and Ph. Salin, Nucl. Phys. B55, 83 (1973).
[13]E. N. Argyres, A. P. Contogouris, J. P. Holden, and M. Svec, Phys. Rev. D 8, 2068 (1973).
[14]I. M. Barbour and R. G. Moorhouse, Nucl. Phys. B69, 637 (1974).
[15]I. S. Barker, A. Donnachie, and J. K. Storrow, Nucl. Phys. B79, 431 (1974).
[16]A. P. Contogouris, Can. J. Phys. 54, 390 (1976).
[17]A. P. Contogouris and M. Svec, Phys. Rev. D 17, 806 (1978).
[18]M. Svec, Lett. Nuovo Cimento 18, 45 (1977); Ph.D. thesis, McGill University (unpublished).
[19]P. Stichel, Z. Phys. 180, 170 (1964); M. Davier, Report No. SLAC-PUB-1529, 1975 (unpublished).
[20]G. F. Chew, M. L. Goldberger, F. E. Low, and Y. Nambu, Phys. Rev. 106, 1345 (1957).
[21]F. A. Berends, A. Donnachie, and D.L. Weaver, Nucl. Phys. B4, 154 (1967).
[22]R. L. Walker, Phys. Rev. 182, 1729 (1969); erratum in R. L. Walker, invited paper, *Fourth International Symposium on Electron and Photon Interactions at*

High Energies, Liverpool, 1969, edited by D. W. Braben and R. E. Rand (Daresbury Nuclear Physics Laboratory, Daresbury, Landeshire, England, 1970).
[23]Y. Hemni *et al.*, Phys. Lett. 43B, 79 (1973).
[24]R. C. E. Devenish, W. A. Rankin, and D. H. Lyth, Phys. Lett. 47B, 53 (1973).
[25]R. G. Moorhouse, H. Oberlack, and A. H. Rosenfeld, Phys. Rev. D 9, 1 (1974); R. G. Moorhouse (private correspondence).
[26]G. Knies, R. G. Moorhouse, and H. Oberlack, Phys. Rev. D 9, 2680 (1974).
[27]R. C. E. Devenish, D. H. Lyth, and W. A. Rankin, Phys. Lett. 52B, 227 (1974).
[28]W. J. Metcalf and R. L. Walker, Nucl. Phys. B76, 253 (1974); R. L. Walker (private correspondence).
[29]R. L. Crawford, Nucl. Phys. B97, 125 (1975).
[30]D. H. Lyth, in *Proceedings of the XVII International Conference on High Energy Physics, London, 1974,* edited by J. R. Smith (Rutherford Laboratory, Chilton, Didcot, Berkshire, England, 1974), p. II-147.
[31]B. Diu and M. LeBellac, Nuovo Cimento 53B, 158 (1968).
[32]W. F. Buhl *et al.*, Phys. Lett. 48B, 388 (1974); V. N. Bolotov *et al.*, *ibid.* 53B, 217 (1974).
[33]B. Wilk, in *Proceedings of the 1971 International Symposium on Electron and Photon Interactions at High Energies, Cornell University*, edited by N. B. Mistry (Laboratory of Nuclear Studies, Cornell University, Ithaca, N. Y., 1972).
[34]G. R. Goldstein, J. F. Owens, and J. P. Rutherford, Nucl. Phys. B57, 18 (1973).
[35]H. Harari, Ann. Phys (N.Y.) 63, 432 (1971).
[36]G. L. Kane and A. Seidl, Rev. Mod. Phys. 48, 309 (1976).
[37]H. P. Jakob, CERN Report No. TH-2022, 1975 (unpublished).
[38]F. Schrempp and B. Schrempp, in *High Energy Physics*, proceedings of the European Physical Society International Conference, Palermo, 1975, edited by A. Zichichi (Editrice Compositori, Bologna, 1976), p. 682.
[39]P. Estabrooks, A. D Martin, Phys Lett. 41B, 83 (1975).
[40]A. C. Irving, Nucl. Phys. B86, 125 (1975).
[41]P. D. B. Collins and A. Fitton, Nucl. Phys. B91, 332 (1975).
[42]R. Thews, G. R. Goldstein, and J. F. Owens, Nucl. Phys. B46, 557 (1972).
[43]E. N. Argyres, A. P. Contogouris, S. Ray, and M. Svec, Nucl. Phys. B45, 267 (1972).
[44]R. P. Worden, Nucl. Phys. B37, 253 (1972).
[45]G. Gault, A. Martin, and G. Kane, Nucl. Phys. B32, 429 (1971).
[46]P. D. B. Collins and A. Fitton, Nucl. Phys. B68, 125 (1974).
[47]E. N. Argyres, A. P. Contogouris, S. Ray, and M. Svec, Ann. Phys. (N.Y.) 85, 283 (1974).
[48]H. K. Armenian, G. R. Goldstein, J. P. Rutherford, and D. L. Weaver, Phys. Rev. D 12, 1278 (1975).
[49]I. S. Barker and J. K. Storrow, Nucl. Phys. B137, 413 (1978).